



# ***Optics in Atmospheric Propagation and Adaptive Systems III***

Anton Kohnle  
John D. Gonglewski  
*Chairs/Editors*

23–24 September 1999  
Florence, Italy

*Sponsored by*

University of Florence, Department of Earth Science (Italy)  
EOS—European Optical Society  
SPIE—The International Society for Optical Engineering  
CNR—The National Research Council of Italy  
NASA—National Aeronautics and Space Administration (USA)  
SIOF—Italian Society of Optics and Photonics  
ASI—The Italian Space Agency

*Published by*

SPIE—The International Society for Optical Engineering



**Volume 3866**

SPIE is an international technical society dedicated to advancing engineering and scientific applications of optical, photonic, imaging, electronic, and optoelectronic technologies.



The papers appearing in this book comprise the proceedings of the meeting mentioned on the cover and title page. They reflect the authors' opinions and are published as presented and without change, in the interests of timely dissemination. Their inclusion in this publication does not necessarily constitute endorsement by the editors or by SPIE.

Please use the following format to cite material from this book:

Author(s), "Title of paper," in *Optics in Atmospheric Propagation and Adaptive Systems III*, Anton Kohnle, John D. Gonglewski, Editors, Proceedings of SPIE Vol. 3866, page numbers (1999).

ISSN 0277-786X  
ISBN 0-8194-3461-2

Published by  
**SPIE—The International Society for Optical Engineering**  
P.O. Box 10, Bellingham, Washington 98227-0010 USA  
Telephone 360/676-3290 (Pacific Time) • Fax 360/647-1445

Copyright ©1999, The Society of Photo-Optical Instrumentation Engineers.

Copying of material in this book for internal or personal use, or for the internal or personal use of specific clients, beyond the fair use provisions granted by the U.S. Copyright Law is authorized by SPIE subject to payment of copying fees. The Transactional Reporting Service base fee for this volume is \$10.00 per article (or portion thereof), which should be paid directly to the Copyright Clearance Center (CCC), 222 Rosewood Drive, Danvers, MA 01923. Payment may also be made electronically through CCC Online at <http://www.directory.net/copyright/>. Other copying for republication, resale, advertising or promotion, or any form of systematic or multiple reproduction of any material in this book is prohibited except with permission in writing from the publisher. The CCC fee code is 0277-786X/99/\$10.00.

Printed in the United States of America.

# Conference Committee

## *Conference Chairs*

**Anton Kohnle**, FGAN Research Institute for Optronics and Pattern  
Recognition (Germany)  
**John D. Gonglewski**, Air Force Research Laboratory (USA)

## *Program Committee*

**Luc R. Bissonnette**, Defence Research Establishment Valcartier (Canada)  
**Piero Brusaglioni**, University of Florence (Italy)  
**Christopher Dainty**, Imperial College of Science, Technology and Medicine (UK)  
**Adam D. Devir**, Institute for Advanced Research and Development (Israel)  
**Marc Séchaud**, ONERA (France)  
**Mikhail A. Vorontsov**, Army Research Laboratory (USA)

## *Session Chairs*

- 1 Characterization of the Propagation Environment  
**Anton Kohnle**, FGAN Research Institute for Optronics and Pattern  
Recognition (Germany)
- 2 Propagation and Imaging Through Inhomogeneous Dense Media  
**Luc R. Bissonnette**, Defence Research Establishment Valcartier (Canada)  
**Piero Brusaglioni**, University of Florence (Italy)
- 3 Propagation and Imaging Through Optical Turbulence  
**Christopher Dainty**, Imperial College of Science, Technology and Medicine (UK)
- 4 Mitigation of Atmospheric Effects and Systems Performance  
**John D. Gonglewski**, Air Force Philips Laboratory (USA)

# Contents

vii *Conference Committee*

## SESSION 1 CHARACTERIZATION OF THE PROPAGATION ENVIRONMENT

---

- 2 **MODTRAN4: radiative transfer modeling for remote sensing (Invited Paper) [3866-02]**  
G. P. Anderson, Air Force Research Lab. (USA); A. Berk, P. K. Acharya, M. W. Matthew, L. S. Bernstein, Spectral Sciences, Inc. (USA); J. H. Chetwynd, Air Force Research Lab. (USA); H. Dothe, S. M. Adler-Golden, Spectral Sciences, Inc. (USA); A. J. Ratkowski, G. W. Felde, Air Force Research Lab. (USA); J. A. Gardner, Air Force Research Lab. (USA) and Univ. of Arizona (USA); M. L. Hoke, Air Force Research Lab. (USA); S. C. Richtsmeier, Spectral Sciences, Inc. (USA); B. Pukall, J. B. Mello, L. S. Jeong, Air Force Research Lab. (USA)
- 11 **Comparison of atmospheric transmittance measurements in the 3- to 5- and 8- to 12- $\mu$ m spectral regions with MODTRAN: considerations for long near-horizontal path geometries [3866-03]**  
A. J. Ratkowski, G. P. Anderson, Air Force Research Lab. (USA); A. D. Devir, Institute for Advanced Research and Development (Israel)
- 23 **High-bandwidth atmospheric-turbulence data collection platform [3866-04]**  
L. J. Otten, Kestrel Corp. (USA); M. C. Roggemann, Michigan Technological Univ. (USA); B. A. Jones, J. Lane, D. G. Black, Kestrel Corp. (USA)
- 33 **SODAR applications for estimating boundary layer parameters [3866-05]**  
A. Capanni, Laboratorio per la Meteorologia e la Modellistica Ambientale (Italy); G. Gualtieri, IATA/CNR (Italy)

## SESSION 2 PROPAGATION AND IMAGING THROUGH INHOMOGENEOUS DENSE MEDIA

---

- 46 **North Oscura Peak laser-imaging polarization experiment [3866-06]**  
D. C. Dayton, S. C. Sandven, Applied Technology Associates (USA); J. D. Goglewski, Air Force Research Lab. (USA)
- 54 **Wavefront propagation and imaging through cirrus clouds [3866-07]**  
B. T. Landesman, P. Kindilien, Applied Technology Associates (USA); C. L. Matson, Air Force Research Lab. (USA)
- 62 **Multispectral IR imaging of point targets in a maritime winter atmosphere [3866-08]**  
K. Stein, FGAN Research Institute for Optronics and Pattern Recognition (Germany)
- 74 **Imaging and localization in turbid media [3866-09]**  
C. L. Matson, Air Force Research Lab. (USA); H. Liu, Univ. of Texas/Arlington (USA); B. T. Landesman, Applied Technology Associates (USA); R. Christopher, Air Force Research Lab. (USA)

- 82 **Phase distortions of sensing beams propagating through aerosols irradiated by power pulse radiation [3866-14]**  
L. K. Chistyakova, Tomsk State Univ. (Russia); R. L. Armstrong, J.-G. Xie, New Mexico State Univ. (USA)
- 88 **Anisoplanatic degradation of correction with real beacon [3866-34]**  
V. P. Lukin, B. V. Fortes, Institute of Atmospheric Optics (Russia)

---

### SESSION 3 PROPAGATION AND IMAGING THROUGH OPTICAL TURBULENCE

---

- 100 **High-resolution imaging through atmospheric turbulence: link between anisoplanatism and intensity fluctuations (Invited Paper) [3866-16]**  
M. Séchaud, F. Mahé, T. Fusco, V. Michau, J.-M. Conan, ONERA (France)
- 110 **Aperture averaging and the temporal spectrum of optical scintillations [3866-17]**  
L. C. Andrews, CREOL/Univ. of Central Florida (USA); R. L. Phillips, C. Y. Hopen, Univ. of Central Florida (USA)
- 119 **Measurements of scintillation over a 17.55-km horizontal path [3866-18]**  
M. Bernhardt, J. W. Buckle, Defence Evaluation and Research Agency Farnborough (UK); C. Dainty, F. Reavell, V. Ruiz-Cortes, Imperial College of Science, Technology and Medicine (UK); M. Welch, Defence Evaluation and Research Agency Farnborough (UK); N. J. Wooder, Imperial College of Science, Technology and Medicine (UK)
- 129 **Fractional moments of low order for scintillation statistics [3866-19]**  
C. Innocenti, Istituto Nazionale per la Fisica della Materia (Italy); A. Consortini, Istituto Nazionale per la Fisica della Materia (Italy) and Univ. of Florence (Italy); F. Rigal, Univ. of Florence (Italy)
- 135 **Measurements of low-level atmospheric turbulence [3866-36]**  
P. M. Blanchard, J. G. Burnett, G. R. G. Erry, D. J. Fisher, A. H. Greenaway, P. Harrison, S. Woods, Defence Evaluation and Research Agency Malvern (UK)

---

### SESSION 4 MITIGATION OF ATMOSPHERIC EFFECTS AND SYSTEMS PERFORMANCE

---

- 144 **Maximum-likelihood constrained regularized algorithms: an objective criterion for the determination of regularization parameters [3866-22]**  
H. Lantéri, M. Roche, O. Cuevas, C. Aime, Univ. de Nice-Sophia Antipolis (France)
- 156 **Generalized seeing monitor (GSM): a dedicated monitor for wavefront optical parameter measurements [3866-24]**  
A. Ziad, F. Martin, R. Conan, J. Borgnino, Univ. de Nice-Sophia Antipolis (France)
- 165 **Photon statistics in adaptive optics [3866-27]**  
M. P. Cagigal, V. F. Canales, Univ. de Cantabria (Spain)
- 176 **Adaptive wavefront correction: a hybrid VLSI/optical system implementing parallel stochastic gradient descent [3866-28]**  
M. H. Cohen, Johns Hopkins Univ. (USA); M. A. Vorontsov, G. W. Carhart, Army Research Lab. (USA); G. Cauwenberghs, Johns Hopkins Univ. (USA)

- 183 **Closed-loop control of a micromachined membrane mirror [3866-29]**  
D. C. Dayton, S. C. Sandven, Applied Technology Associates (USA); J. D. Gonglewski, Air Force Research Lab. (USA)
- 192 **Optical communication link with an adaptive transmitter based on interference metric optimization [3866-30]**  
J. C. Ricklin, Army Research Lab. (USA); F. M. Davidson, Johns Hopkins Univ. (USA)
- 198 **Use of dual-wavelength dynamic holography in adaptive optics [3866-31]**  
V. Yu. Venediktov, V. A. Berenberg, A. A. Leshchev, M. V. Vasil'ev, Institute for Laser Physics (Russia); M. T. Gruneisen, Air Force Research Lab. (USA)
- 207 **Distinctions and common features of two schemes of laser guide star formation [3866-32]**  
V. P. Lukin, Institute of Atmospheric Optics (Russia)
- 217 **Experimental limits on curvature sensing [3866-35]**  
E. N. Ribak, Technion—Israel Institute of Technology

---

**ADDITIONAL PAPER FROM SESSION 2**

- 222 **High-sensitivity DIAL measurements with spectrally coherent infrared lasers [3866-37]**  
V. Hasson, K. Kovacs, Texton Systems Corp. (USA)
- 236 *Author Index*

## **SESSION 1**

### **Characterization of the Propagation Environment**

## MODTRAN4: Radiative transfer modeling for remote sensing

G. P. Anderson<sup>a</sup>, A. Berk<sup>b</sup>, P. K. Acharya<sup>b</sup>, M. W. Matthew<sup>b</sup>, L. S. Bernstein<sup>b</sup>, J. H. Chetwynd<sup>a</sup>,  
H. Dothe<sup>b</sup>, S. M. Adler-Golden<sup>b</sup>, A. J. Ratkowski<sup>a</sup>, G. W. Felde<sup>a</sup>,  
J. A. Gardner<sup>a,c</sup>, M. L. Hoke<sup>a</sup>, S. C. Richtsmeier<sup>b</sup>, B. Pukall<sup>a</sup>, J. Mello<sup>a</sup> and L. S. Jeong<sup>a</sup>

<sup>a</sup> Air Force Research Laboratory, Space Vehicles Directorate, Hanscom AFB 01731

<sup>b</sup> Spectral Sciences, Inc., Burlington, MA 01803

<sup>c</sup> University of Arizona, Tucson, AZ 85721

### ABSTRACT

MODTRAN4, the newly released version of the U.S. Air Force atmospheric transmission, radiance and flux model is being developed jointly by the Air Force Research Laboratory / Space Vehicles Directorate (AFRL / VS) and Spectral Sciences, Inc. It is expected to provide the accuracy required for analyzing spectral data for both atmospheric and surface characterization. These two quantities are the subject of satellite and aircraft campaigns currently being developed and pursued by, for instance: NASA (Earth Observing System), NPOESS (National Polar Orbiting Environmental Satellite System), and the European Space Agency (GOME – Global Ozone Monitoring Experiment). Accuracy improvements in MODTRAN relate primarily to two major developments: (1) the multiple scattering algorithms have been made compatible with the spectroscopy by adopting a correlated- $k$  approach to describe the statistically expected transmittance properties for each spectral bin and atmospheric layer, and (2) radiative transfer calculations can be conducted with a Beer-Lambert formulation that improves the treatment of path inhomogeneities. Other code enhancements include the incorporation of solar azimuth dependence in the DISORT-based multiple scattering model, the introduction of surface BRDF (Bi-directional Radiance Distribution Functions) models and a  $15\text{ cm}^{-1}$  band model for improved computational speed.

**KEYWORDS:** MODTRAN, Remote sensing, Surface Albedos, Aerosols, Multiple Scattering

### 1. MODTRAN

The new MODTRAN4 radiative transfer code, with its correlated- $k$  Beer's Law algorithm<sup>2,3</sup>, can efficiently and accurately calculate the scattering and absorption signatures of realistic molecular, aerosol and cloudy environments in the lower and middle atmosphere. The current approach for molecular absorption accommodates line overlap and partial correlations between both molecular species and the solar irradiance, while maintaining internal band model spectral resolution at either  $1\text{ cm}^{-1}$  or  $15\text{ cm}^{-1}$  binning. This new level of code evolution and validation will permit improved syntheses, analyses and detection of total (direct plus scattered) solar and thermal energy components for clouds, aerosol decks, plumes and other realistic non-clear sky conditions.

Validation is typically provided through two avenues. The first involves direct comparisons with line-by-line calculations, as exemplified by FASE (FASCODE for the Environment)<sup>4</sup>. DoD and DOE jointly developed the FASE line-by-line (LBL) algorithm from FASCODE<sup>5</sup> with its optimized line-shape decomposition algorithm<sup>6</sup>. FASE can be considered the molecular standard for layer effective optical depths, single scattering albedos, and transmittances. Direct comparisons with FASE enable the MODTRAN4 algorithm to be refined for more flexible spectral resolution plus efficient and accurate determination of those layer quantities necessary for multiple scattering applications; e.g. DISORT<sup>7</sup> and a simpler 2-stream model<sup>8</sup>. The second validation step centers on comparisons against a variety of measurements, including airborne sensors like AVIRIS<sup>9</sup>, in the visible through short-wave infrared (SWIR), and HIS (High Resolution Interferometric Spectrometer<sup>10,11</sup>), in the mid-wave and long-wave infrared (MWIR – LWIR), both under both clear and clouded skies.

Besides the correlated- $k$  initiative, MODTRAN4<sup>2</sup> now includes major model enhancements in three additional areas. First, ground surface modeling has been upgraded to couple the atmospheric radiative transport with surface terrain BRDFs (Bidirectional Reflectance Distribution Functions). This includes options for modeling surface adjacency effects. Second, the DISORT discrete ordinate multiple scattering (MS) model now includes an azimuth dependence in the solar scattered component. Third, an optimized, reduced spectral resolution ( $15\text{ cm}^{-1}$ ) band model option has been introduced as an

alternative to the standard MODTRAN 1 cm<sup>-1</sup> band model for increased speed when the higher spectral resolution is unnecessary.

## 1.1 ADDITION OF A CORRELATED-*k* (CK) CAPABILITY TO MODTRAN

The new CK capability in MODTRAN<sup>3</sup> provides an accurate and fast means for evaluating the effects of clouds and heavy aerosol loading on retrievals (both surface properties and species concentration profiles) and on atmospheric radiative heating/cooling calculations. These radiative transfer computations require coupling the effects of gaseous molecular absorption due primarily to water vapor, carbon dioxide, and ozone, with particulate multiple scattering due to aerosols, ice crystals, and water droplets. In order to adapt a band model approach for use in scattering calculations it is necessary to express the band model transmission function in terms of a weighted sum of Beer's law exponential terms. Thus, a method for determining the weighing factors and monochromatic absorption coefficients for the MODTRAN band model is required. An abbreviated discussion of the CK approach as tailored for integration into MODTRAN is given below; for a more complete discussion of the CK method the reader is referred to Lacis and Oinas<sup>1</sup>.

Consider the problem of determining the average transmittance, as defined by Beer's law, for a homogeneous path over a finite spectral interval. The generalization to inhomogeneous paths is straightforward. The path transmittance can be exactly determined through evaluation of:

$$T(u) = \frac{I}{\omega_2 - \omega_1} \int_{\omega_1}^{\omega_2} e^{-k(\omega)u} d\omega \quad ,$$

where  $\omega$  is frequency,  $k(\omega)$  is the monochromatic absorption coefficient, and  $u$  is absorber column density. The basis of the CK approach is that evaluation of  $T(u)$  by integration over frequency can be replaced by an equivalent integration over the distribution of absorption coefficient values  $f(k)$  in the spectral interval

$$T(u) = \int_0^{\infty} f(k) e^{-ku} dk \quad .$$

The distribution function  $f(k)$  is not smooth or monotonic; it generally consists of a series of sharp spikes which reflect the sharp line structure of  $k(\omega)$ . It then becomes more computationally convenient to work with the smooth and monotonic cumulative probability distribution function

$$g(k) = \int_0^k dk' f(k') \quad .$$

where  $k(g)$  is given by the inverse of  $g(k)$ ,  $k(g) = g^{-1}(k)$ .

The MODTRAN band model for a single species is based on four parameters: (1) the integrated line strength  $S$  in a spectral interval  $\Delta\omega$  ( $\Delta\omega = 1$  cm<sup>-1</sup> in MODTRAN), (2) the effective number of equivalent lines  $n$  (non-integer values of  $n$  are acceptable) in the interval, (3) the average pressure broadening Lorentz line width  $\gamma_L$ , and (4) the Doppler line width  $\gamma_D$ . These parameters are determined directly from the 1996 HITRAN<sup>12</sup> parameter line compilation.

## 1.2 MODTRAN MULTIPLE SCATTERING

For monochromatic radiation, the transmittance through two path segments is the product of the two individual segment transmittances, i.e., Beer's Law is obeyed. However, this multiplicative relationship between layer transmittances breaks down for molecular band models. The product of *spectrally integrated* path transmittances is not equal to the coupled path transmittance spectrally integrated due to the strong molecular spectral line structure. This is problematic because multiple scattering models such as those in MODTRAN couple intrinsic layer flux calculations assuming Beer's Law. To solve this problem, correlated-*k* algorithms recast band model radiative transport into a weighted sum of monochromatic radiative transport problems. In MODTRAN, the distribution of molecular absorption coefficients, i.e., the *k*-distributions required for the correlated-*k* implementation, are statistical representations based on band model parameters. They are not the actual distributions at a given wavelength, temperature and pressure for any given spectral bin. The MODTRAN *k*-distribution database is a relatively small table which only depends on the effective number of lines in a spectral bin and the Lorentz and

Doppler half-widths. MODTRAN interpolates over this table for each spectral frequency bin to determine the  $k$  distribution appropriate for each layer.

The importance of the correlated- $k$  algorithm in MODTRAN MS calculations can be demonstrated by comparing long-wave cooling rate calculations performed both with and without the algorithm. Results are illustrated in Figure 1. Cooling rates are proportional to the derivative of net flux with respect to pressure<sup>13,14</sup>. In the LWIR, the MS contribution to atmospheric path radiance is generally small. Therefore, thermal flux at any altitude can be computed by explicitly integrating thermal emission for lines-of-sight spanning the upward and downward hemispheres. These calculations do not rely on a Beer's Law dependence. Hicke *et al.*<sup>15</sup> used this approach to generate the cooling rate curve labeled MOD3 LOS in Figure 1 and compared the results to broad band model RRTM<sup>16</sup> (Rapid Radiative Transfer Model) predictions. Alternatively, fluxes can be computed directly from the MS models, which couple together layer contributions assuming the Beer's Law dependence. The results of these calculations are included in Figure 3, both with and without the correlated- $k$  option and for both the approximate 2-stream and the DISORT MS model. These curves demonstrate that the correlated- $k$  algorithm is required to correctly compute the LWIR fluxes.

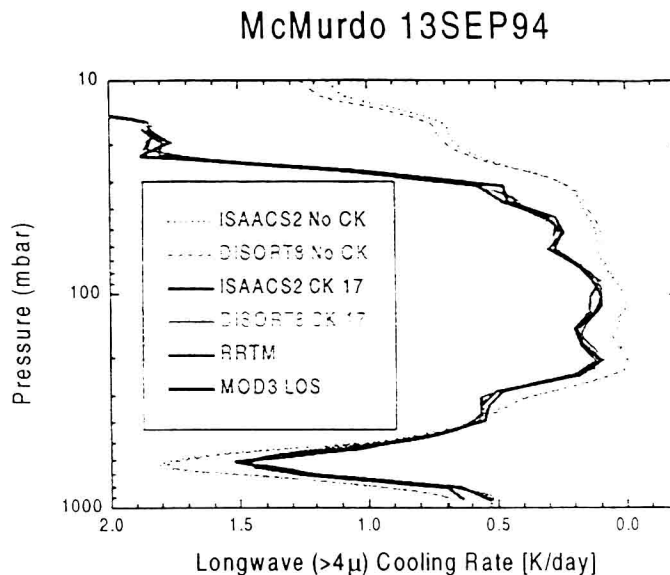


**Figure 1:** Longwave Cooling Rates for September 13, 1994, McMurdo Station. MODTRAN4 results are compared to the predictions from Hicke, *et al.*<sup>15</sup> The darker lines represent the better physics for determining flux differentials and subsequent cooling rates.

Another major upgrade in the MODTRAN4 multiple scattering treatment is the inclusion of relative solar azimuth dependence through a new interface to the DISORT algorithm. While the MODTRAN single scatter algorithm has always included azimuth dependence as well as spherical refractive geometry effects, the original interface to DISORT allowed it to calculate only an *azimuth independent* solar source function for each layer. MODTRAN now incorporates this source function into its LOS radiance integration (essentially multiplying it by foreground transmittance and layer emissivity along the LOS). In the new integration, MODTRAN backs out the solar MS layer radiances directly from the DISORT *azimuth-dependent* solar radiances, not from the source function. MODTRAN then computes plane-parallel single scatter solar radiances and subtracts them from the DISORT radiances to isolate the MS contributions.

### 1.3 Ground Surface Enhancements

The major radiometric modification to the MODTRAN surface treatment is the coupling of the atmospheric radiative transport to a surface BRDF. Seven vegetation canopy BRDF models have been incorporated into MODTRAN. Two of the BRDF models are strictly empirical, the Walthall model<sup>17</sup> in its symmetric form and the symmetric Sinusoidal-Walthall model (obtained from the Walthall form by replacing the zenith angles in radians with their sine function). Only these first two will be discussed. The others are semi-empirical or physics-based algorithms and are described in the MODTRAN4 documentation.

In MODTRAN, integrals over the surface BRDF are numerically computed on the input spectral grid for coupling to the atmospheric radiative transport. For the *imaged-pixel*, three BRDF derived quantities are required:

- the BRDF value at the solar and viewing angles, for the reflected direct solar flux calculations;
- the LOS directional emissivity, for the surface thermal emission calculations; and
- the LOS directional reflectivity, for the reflected solar and thermal diffuse flux calculations.

The diffuse downward surface flux is modeled as being isotropically distributed for the reflected flux calculations. MODTRAN provides two model options for computing multiple scattering contributions, an approximate 2-stream algorithm and the DISORT N-stream model. If the 2-stream model is selected, the surface albedo and solar-direction directional reflectivity are obtained by integrating over the *area-averaged* surface BRDF. This later integral is used to reflect the direct solar irradiance off the ground as a component of the lower boundary condition.

A full coupling of DISORT with the *area-average* surface BRDF could be performed by computing directional emissivity and azimuth moment integrals at the N double-quadrature polar (zenith) angles and for the solar and view directions. However, in version 1.0, the *area-averaged* surface used in DISORT is modeled as a Lambertian reflector with the albedo calculated from the input BRDF.

The importance of a canopy BRDF is demonstrated in Figure 2. Calculations were performed for a red (650-nm) band in the visible spectral region with 23-km ground visibility, with a 50° solar zenith angle, and with a 20° off-nadir sensor viewing angle at 20-km altitude. Initially, the observed radiance as a function of *surface* relative solar azimuth (180° corresponds to the sensor looking towards the sun) was computed for a Lambertian surface. The surface albedo was set equal to the sensor view angle directional reflectivity of the canopy BRDF. As the surface relative solar azimuth increases from 0 to 180°, the scattering angle decreases from 150 to 110°. Thus, the single scatter Rayleigh component decreases with increasing relative azimuth while the aerosol scattering component increases as the forward direction is approached. The minimum radiance occurs at a surface relative solar azimuth near 70°, and the maximum occurs in the forward scattering direction. The location of the maximum radiance switches when a Walthall BRDF obtained from a fit of radiance measurements for 4" alfalfa cropland is inserted into the MODTRAN calculation. Due to the hot spot reflectance, the parameterized BRDF is largest in the backscatter direction, when the surface relative solar azimuth angle is near 0°.

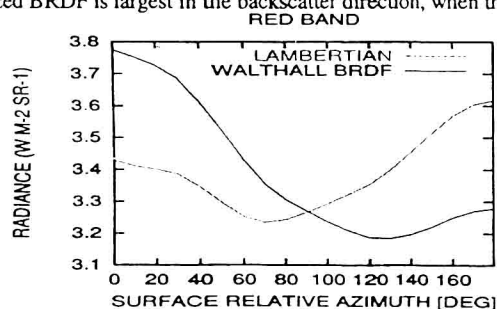


**Figure 2:** MODTRAN4 In-Band (650 nm) Radiance Relative Azimuth Dependence. The maximum occurs in the forward scattering direction (180°) for the Lambertian surface and in the backscatter direction for the parameterized BRDF. See text for discussion.

#### 1.4 MODTRAN 15 cm<sup>-1</sup> Band Model

A 15 cm<sup>-1</sup> band model has been introduced into MODTRAN4 as a fast alternative to the standard MODTRAN 1 cm<sup>-1</sup> band model. Initially, the new band model was created by generating a 15 cm<sup>-1</sup> band model database and by computing band model transmittances exactly as is done for the 1 cm<sup>-1</sup> model. This approach produced too much absorption, Figure 3a. A basic premise of the MODTRAN 1 cm<sup>-1</sup> band model is that lines within a spectral interval can be modeled as randomly distributed. Often, few (1 or 2) lines dominate the absorption in a 1 cm<sup>-1</sup> interval; and, if many lines do contribute, they still tend to be nearly randomly distributed. This is not true with the wider bandwidth. In a 15 cm<sup>-1</sup> interval, molecular lines are generally clumped together more than a random distribution would predict, and these clumped lines cannot absorb as much as they would if they were spread out.

To adjust the model, the calculation of the 15 cm<sup>-1</sup> line spacing band model parameters has been tied to the 1 cm<sup>-1</sup> band model. For each molecular species that absorbs in a specified 15 cm<sup>-1</sup> spectral band, the homogeneous layer column amount that produces an in-band transmittance of  $\exp(-1)$  – where the band model pseudo optical depth is unity – is calculated. The transmittance is determined by averaging 15 MODTRAN 1 cm<sup>-1</sup> band model calculations. In a subsequent calculation using the 15 cm<sup>-1</sup> band model, the line spacing band model parameter is tuned to produce the same transmittance. All these calculations are performed for a fixed grid of temperatures and at 1.0-atm pressure for H<sub>2</sub>O, at 0.2-atm pressure for O<sub>3</sub>, and at 0.4-atm pressure for all other species. The selection of pressures is based on the vertical distribution of each species – H<sub>2</sub>O is peaked near the surface, ozone peaks just above the troposphere, and the densities of the uniformly mixed gases are proportional the total atmospheric density. The results are illustrated for a vertical path from the ground to space in Figure 3b (LWIR - MWIR) and Figures 4a and 4b (SWIR - NIR). The residuals are generally at the percent level or lower, and the bias toward too much absorption is eliminated.

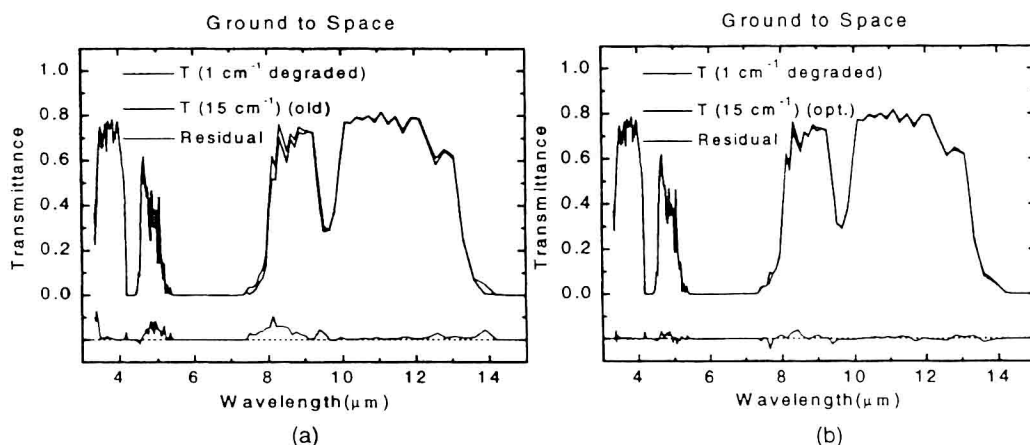


**Figure 3:** Comparison of MODTRAN 1 cm<sup>-1</sup> and 15 cm<sup>-1</sup> Band Model LWIR / MWIR Spectral Transmittances (a) Before and (b) After Tuning of the 15 cm<sup>-1</sup> Line Spacing Band Model Parameters. All comparisons are performed with a 15 cm<sup>-1</sup> rectangular slit function.

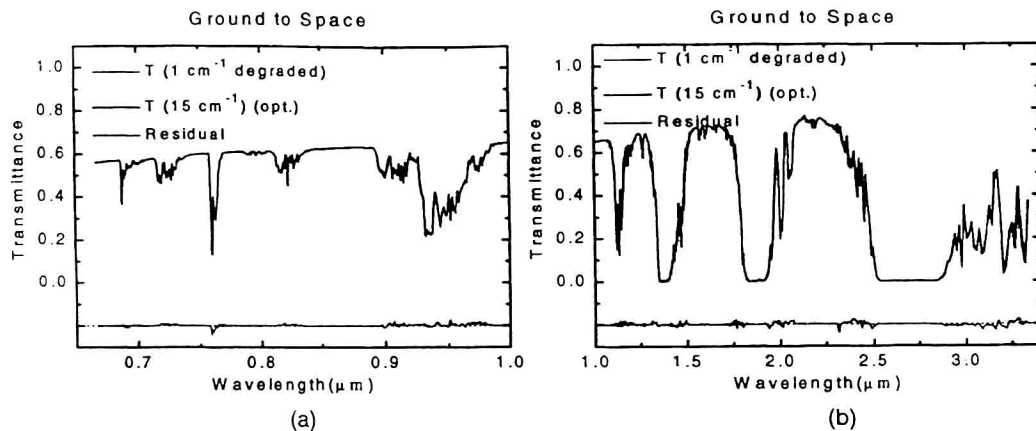


**Figure 4:** Comparison of MODTRAN 1 cm<sup>-1</sup> and 15 cm<sup>-1</sup> Band Model (a) NIR and (b) SWIR Spectral Transmittances. All comparisons are performed with a 15 cm<sup>-1</sup> rectangular slit function.

## 2. ATMOSPHERIC CORRECTION ALGORITHM

A MODTRAN4-based "atmospheric correction algorithm" (ACA) is also being developed. The intent is to provide accurate surface reflectance and emissivity images, effectively removing the atmospheric component. The main objectives are to include (1) physics-based descriptions of surface and atmospheric properties (such as surface albedo, relative altitude, water vapor column, aerosol and cloud optical properties, and temperatures), (2) minimal computational time requirements, and (3) user-friendly interface for generating MODTRAN4-based look-up tables.

Validation and development exercises are being carried out on AVIRIS data with the additional expectation of having a system compatible with the NASA Earth Observing System optical measurements. The algorithm for deriving the surface and atmospheric properties utilizes the full MODTRAN4 accuracy (thermal and solar) and accounts for adjacency effects associated with atmospheric scattering. Compared to previous versions of MODTRAN, the new correlated-*k* radiative transfer algorithm provides improvements in implementation of multiple scattering, especially under conditions of partial cloud and/or aerosol contamination.

The new ACA draws heavily on existing spectral analysis methods and codes that have been developed for both research and general use<sup>18-22</sup>. It is designed as a general-purpose code and is evolving in parallel with upgrades to MODTRAN in order to take advantage of the latest improvements in accuracy and speed. The ACA is now interfaced with a final version of MODTRAN4.

The initial version of the ACA provides the following capabilities:

- An analysis tool to support AVIRIS and similar spectral imaging sensors;
- A graphical user interface for performing MODTRAN4 spectral calculations, including data simulations, creating the essential look-up tables upon which the algorithm is based.

On output the ACA provides:

- Data-derived column water vapor and relative surface altitude (from column oxygen) image maps, and aerosol property retrieval capability based on known surface reflectances;
- Atmospherically corrected images (i.e., surface spectral reflectance cubes, with the H<sub>2</sub>O, O<sub>2</sub>, CO<sub>2</sub>, and aerosol dependence removed) for non-thermal wavelengths (mid-IR through UV), including image-sharpening corrections.

### 2.1 ACA METHODOLOGY

As in other first-principles atmospheric correction codes, model simulations of the spectral radiance are performed for appropriate atmospheric and viewing conditions over a range of surface reflectances. The desired properties (reflectance,

column water vapor, etc.) are derived from the spectral radiance at each image pixel using look-up tables that are generated from these simulations. To minimize the number of simulations (i.e., MODTRAN runs) required to generate the tables, a physics-based parameterization of the radiance-reflectance relationship is used. This relationship can vary across the scene due to variations in water vapor column density and relative altitude. Therefore, as in the ATREM code<sup>18</sup>, the water vapor column is first determined for each pixel, then the result is used as an input to the surface reflectance retrieval algorithm.

Initially the ACA addresses the mid-IR through UV wavelengths where thermal emission can be neglected. For this situation the spectral radiance  $L^*$  at a sensor pixel may be parameterized as (after<sup>23,24</sup>):

$$L^* = Ap/(1-p_e S) + Bp_e/(1-p_e S) + L_a^* \quad (1)$$

where  $p$  is the pixel surface reflectance,  $p_e$  is an average surface reflectance for the surrounding region,  $S$  is the spherical albedo of the atmosphere,  $L_a^*$  is the radiance backscattered by the atmosphere, and  $A$  and  $B$  are coefficients that depend on atmospheric and geometric conditions. The first term in Equation (1) corresponds to the radiance from the surface that travels directly into the sensor, while the second term corresponds to the radiance from the surface that is scattered by the atmosphere into the sensor.

The values of  $A$ ,  $B$ ,  $S$ , and  $L_a^*$  may be determined empirically from MODTRAN spectral radiance calculations for three different spatially and spectrally uniform reflectances (such as  $p=p_e=0, 0.5$ , and  $1.0$ ). The backscattered radiance term  $L_a^*$  is simply the radiance for zero surface reflectance ( $p=p_e=0$ ). The first (direct radiance) term is output by MODTRAN separately from the total radiance  $L^*$ ; thus, the second (scattered radiance) term is isolated by subtracting the direct surface radiance and  $L_a^*$  from the total radiance. Equation (1) applies rigorously to monochromatic light. However, because  $S$  is small (of order  $10^{-2}$  to  $10^{-1}$  for clear sky) the radiance-reflectance relationship is sufficiently linear that Equation (1) accurately describes integrated in-band (i.e., sensor channel) radiances as well as true monochromatic radiance.

The spatially averaged reflectance  $p_e$  is used to account for "adjacency effects"—i.e., radiance contributions that, because of atmospheric scattering, originate from parts of the surface not in the direct line of sight. Strictly speaking, the  $p_e$ 's in the numerator of the second term and in the denominators of the first and second terms are not identical. The former represents a weighted average over the surface region (typically around 1 km in diameter when viewed from a high-altitude sensor) that contributes to forward scattering from the ground into the sensor. The latter represents an average over a larger region that contributes to the scattering back down to the ground. However, because  $S$  is small and the size of the averaging region is non-critical, the two averaged reflectances may be equated with little error.

The method for solving Equation (1) for the surface reflectance  $p$  parallels that in the ATCOR2 code<sup>21</sup> but differs in detail. MODTRAN4 spectral radiance calculations for surface reflectances of 0, 0.5, and 1.0 are performed for a range of water vapor column densities to determine the Equation (1) parameters as a function of wavelength and water vapor column. The parameters for a spectral interval containing a selected water band are used to determine water vapor column densities for each pixel. The method, which is an extension of the two-band method used in ATREM<sup>18</sup>, involves comparisons of data and simulations for in-band and out-of-band radiance averages using a look-up table.

In addition to determining the water vapor column density, the ACA derives pressure altitudes by applying the same method to the oxygen 762 nm absorption band. Because MODTRAN4's correlated- $k$  algorithm more accurately represents molecular absorption in the presence of scattering, the derived water vapor and oxygen densities are expected to be more accurate than those obtained using previous versions of MODTRAN as well as from more approximate radiation transfer algorithms. Other bands of  $O_2$  and  $CO_2$  will also be examined for improved accuracy in altitude definition across the image.

### 3. RESULTS

Several AVIRIS images have been analyzed to test the ACA. Figure 5 demonstrates the ability of the ACA to sharpen an image by 'removing' the intervening atmosphere. In addition, a simulation capability of the ACA has been employed. The original radiance image (available from <http://makalu.jpl.nasa.gov>) was first reduced to reflectance, then the intervening atmosphere (originally quite dry and clear) was replaced by a 5 km visibility and high humidity. The resultant simulated radiance image, shown in (a) is very hazy, but still a potentially realistic scenario. This image was then processed with the ACA to see if it could reproduce the original reflectance image. The results, both with and without adjacency effect compensation, are shown in (b) and (c); the latter is in excellent agreement with the original reflectance. While these

figures show only red-green-blue representations of the data, the actual data and reconstructions are spectra that cover the full 400-2500 nm region of the sensor.

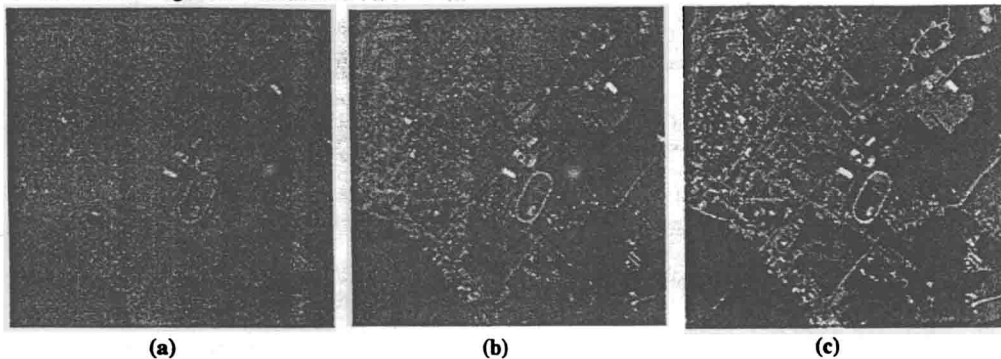


**Figure 5 a, b, and c:** 5a is an AVIRIS image 'contaminated' with high aerosol loading and relative humidity; 5b is the simple reflectance reconstruction using the ACA without adjacency compensation; 5c includes adjacency effects.

#### 4. CONCLUSION

Development of the ACA, a fast software package for atmospheric correction and modeling of spectral images using MODTRAN4, has begun with a focus on sensors covering the 0.4 to 2.5  $\mu\text{m}$  wavelength range. Initially the algorithm has been applied to AVIRIS data. Future efforts will focus on accuracy evaluations, improvements to MODTRAN4, incorporation of aerosol retrieval techniques, and on extension to the thermal IR region.

#### 5. ACKNOWLEDGEMENT

The work at Spectral Sciences was supported by the US Air Force Contract no. F19628-91-C-0145. This paper has been specifically drawn from many recent 'manuscripts-in-progress', with principal authorships by A. Berk, S. Adler-Golden, P.K. Acharya, G. Felde and J. Gardner. GPA wishes to thank them all for lending their texts for this purpose.

#### 6. REFERENCES

1. A. A. Lacis and V. Oinas, "A description of the Correlated K Distribution Method for Modeling Nongray Gaseous Absorption, Thermal Emission, and Multiple Scattering in Vertically in Homogeneous Atmospheres," *J. Geophys. Res.*, 96, 9027 - 9063, 1991.
2. A. Berk, L.S. Bernstein, G.P. Anderson, P.K. Acharya, D.C. Robertson, J.H. Chetwynd and S.M. Adler-Golden, "MODTRAN Cloud and Multiple Scattering Upgrades with Application to AVIRIS", *Remote Sens. Environ.* 65:367-375, 1998.
3. L.S. Bernstein, A. Berk, D.C. Robertson, P.K. Acharya, G.P. Anderson, and J.H. Chetwynd, "Addition of a Correlated- $k$  Capability to MODTRAN", *Proc. IRIS Targets, Backgrounds and Discrimination*, Vol. II, 239-248 1996.
4. H.E. Snell, G.P. Anderson, J. Wang, J.-L. Moncet, J.H. Chetwynd, S.J. English, Validation of FASE (FASCODE for the Environment) and MODTRAN3: Updates and Comparisons with Clear-Sky Measurements, The European Symposium on Satellite Remote Sensing, Conference on Passive Infrared Remote Sensing of Clouds and the Atmosphere III, *Proceedings of SPIE*, Paris, France, 1995.
5. S. A. Clough, F. X. Kneizys, G. T. Anderson, E. P. Shettle, J. H. Chetwynd, L. W. Abreu, and L. A. Hall, "FASCODE3 Spectral Simulation" *Proceedings of the International Radiation Symposium*, Lenoble and Geleyn, Deepak Publishing, 1988.
6. S.A. Clough and F.X. Kneizys, Convolution Algorithm for the Lorentz Function, *Appl. Opt.*, 18, 2329, 1979.
7. K. Stamnes, S.-C. Tsay, W. Wiscombe, and K. Jayaweera, "Numerically Stable Algorithm for Discrete-Ordinate-Method Radiative Transfer in Multiple Scattering and Emitting Layered Media", *Applied Optics*, 27, 2502-2509, 1988.
8. R. G. Isaacs, W. C. Wang, R. D. Worsham, and S. Goldenberg, "Multiple Scattering LOWTRAN and FASCODE Models," *Applied Optics*, 26, 1272-1281, 1987.

9. R.O. Green, B. Pavri, J. Faust, O. Williams, C. Chovit, "Inflight validation of AVIRIS Calibration in 1996 and 1997, Summaries of the Seventh Annual JPL Airborne Earth Science Workshop, JPL Publication 97-21, Vol. 1, Pasadena, California, pp. 193-203, 1998.
10. W.L. Smith, H.E. Revercomb, R.O. Knuteson, F.A. Best, R. Dedecker, H.B. Howell, and H.M. Woolf, Cirrus Cloud Properties Derived from High Resolution Infrared Spectrometry during FIRE ii. Part I: The High Resolution Interferometer Sounder (HIS) Systems, *Journal of the Atm. Sciences*, 52, 4238-4245, 1995.
11. J. Wang, G.P. Anderson, H.E. Revercomb, and R.O. Knuteson, Validation of FASCOD3 and MODTRAN3: Comparison of Model Calculations with Ground-Based and Airborne Interferometer Observations Under Clear-Sky Conditions, *Appl. Optics*, 35, 1996.
12. L.S. Rothman, *et al.*, 1996, "The HITRAN Molecular Database: Edition of 1996," Released as a CD-Rom, June, 1996. ('rothman@plh.af.mil') and L.S. Rothman, C.P. Rinsland, A. Goldman, S.T. Massie, D.P. Edwards, J.-M. Flaud, A. Perrin, C. Camy-Peyret, V. Dana, J.-Y. Mandin, J. Schroeder, A. McCann, R.R. Gamache, R.B. Wattson, K. Yoshino, K.V. Chance, K.W. Jucks, L.R. Brown, V. Nemtchinov, and P. Varanasi, "The HITRAN Molecular Spectroscopic Database and HAWKS (HITRAN Atmospheric Workstation): 1996 Edition," *J. Quant. Spectrosc. Radiat. Transfer*, Vol. 60, pp. 665-710, 1998.
13. S.A. Clough, M.J. Iacono, J.-L. Moncet, "Line-by-Line Calculations of Atmospheric Fluxes and Cooling Rates: Applications to Water Vapor", *J. Geophys. Res.*, 97, 15761, 1992.
14. L.S. Bernstein, A. Berk, P.K. Acharya, D.C. Robertson, G.P. Anderson, J.H. Chetwynd and L.M. Kimball, "Very Narrow Band Model Calculations of Atmospheric Fluxes and Cooling Rates", *Journal of Atmospheric Sciences*, Vol. 53, No. 19, pp. 2887-2904, 1996.
15. J. Hicke, A. Tuck, and H. Vomel, "Lower Stratospheric Radiative Heat Rates and Sensitivities Calculated from Antarctic Balloon Observations", *J. Geophys. Res.*, 104D, 9293-9308, 1999.
16. E.J. Mlawer, S.J. Taubman, P.D. Brown, M.J. Iacono, and S.A. Clough, "Radiative Transfer for Inhomogeneous Atmospheres: RRTM, a Validated Correlated-k Model for the Longwave", *J. Geophys. Res.*, 102, 16,663-16,682, 1996.
17. C.L. Walthall, J.M. Norman, J.M. Welles, G. Campbell, and B.L. Blad, "Simple Equation to Approximate the Bidirectional Reflectance from Vegetative Canopies and Bare Soil Surfaces", *Applied Optics*, 24, 383-387, 1985.
18. B.-C. Gao, K.B. Heidebrecht, and A.F.H. Goetz, "Atmosphere Removal Program (ATREM) Version 2.0 Users Guide," Center for the Study of Earth from Space/CIRES, University of Colorado, Boulder, Colorado, 26 pages, 1996.
19. R.O. Green, D.A. Roberts, and J.E. Conel, "Characterization and Compensation of the Atmosphere for Inversion of AVIRIS Calibrated Radiance to Apparent Surface Reflectance," Summaries of the Sixth Annual JPL Airborne Earth Science Workshop, JPL Publication 96-4, Vol. 1, Pasadena, California, pp. 135-146, 1996.
20. M. D. King, Y. J. Kaufman, W. P. Menzel, and D. Tanre, "Remote Sensing of Cloud, Aerosol, and Water Vapor Properties from the Moderate Resolution Imaging Spectrometer (MODIS)," *IEEE Transactions on Geoscience and Remote Sensing*, Vol. 30, pp. 2-27, 1992.
21. R. Richter, "Atmospheric Correction of DAIS Hyperspectral Image Data," SPIE AEROSENSE '96 Conference, Orlando, FL, April 8-12, SPIE Proceedings, Vol. 2758, 1992.
22. K. Staenz, D.J. Williams, and B. Walker, "Surface Reflectance Retrieval from AVIRIS Data Using a Six-Dimensional Look-Up Table," *Summaries of the Sixth Annual JPL Airborne Earth Science Workshop*, March 4-8, 1996, JPL Publication 96-4, Vol. 1, Pasadena, California, pp. 223-229, 1996.
23. E.F. Vermote, N. El Saleous, C.O. Justice, Y.J. Kaufman, J.L. Privette, L. Remer, J.C. Roger, and D. Tanre, "Atmospheric Correction of Visible to Middle-Infrared EOS-MODIS Data Over Land Surfaces: Background, Operational Algorithm and Validation," *J. Geophys. Res.*, Vol. 102, pp. 17131-17141, 1997.
24. D.J. Williams, A. Royer, N.T. O'Neill, S. Achal, and G. Weale, "Reflectance Extraction from CASI Spectra Using Radiative Transfer Simulations and a Rooftop Radiance Collector," *Can. Journal of Remote Sensing*, Vol. 18, pp. 251-261, 1992.